

University of Groningen

Observation of the Annihilation Decay Mode $B^0 \rightarrow K^+ K^-$

LHCb Collaboration

Published in:
Physical Review Letters

DOI:
[10.1103/PhysRevLett.118.081801](https://doi.org/10.1103/PhysRevLett.118.081801)

IMPORTANT NOTE: You are advised to consult the publisher's version (publisher's PDF) if you wish to cite from it. Please check the document version below.

Document Version
Publisher's PDF, also known as Version of record

Publication date:
2017

[Link to publication in University of Groningen/UMCG research database](#)

Citation for published version (APA):

LHCb Collaboration (2017). Observation of the Annihilation Decay Mode $B^0 \rightarrow K^+ K^-$. *Physical Review Letters*, 118(8), [081801]. <https://doi.org/10.1103/PhysRevLett.118.081801>

Copyright

Other than for strictly personal use, it is not permitted to download or to forward/distribute the text or part of it without the consent of the author(s) and/or copyright holder(s), unless the work is under an open content license (like Creative Commons).

The publication may also be distributed here under the terms of Article 25fa of the Dutch Copyright Act, indicated by the "Taverne" license. More information can be found on the University of Groningen website: <https://www.rug.nl/library/open-access/self-archiving-pure/taverne-amendment>.

Take-down policy

If you believe that this document breaches copyright please contact us providing details, and we will remove access to the work immediately and investigate your claim.

Downloaded from the University of Groningen/UMCG research database (Pure): <http://www.rug.nl/research/portal>. For technical reasons the number of authors shown on this cover page is limited to 10 maximum.



Observation of the Annihilation Decay Mode $B^0 \rightarrow K^+ K^-$

R. Aaij *et al.**

(LHCb Collaboration)

(Received 27 October 2016; published 21 February 2017)

A search for the $B^0 \rightarrow K^+ K^-$ decay is performed using pp -collision data collected by LHCb. The data set corresponds to integrated luminosities of 1.0 and 2.0 fb⁻¹ at center-of-mass energies of 7 and 8 TeV, respectively. This decay is observed for the first time, with a significance of more than 5 standard deviations. The analysis also results in an improved measurement of the branching fraction for the $B_s^0 \rightarrow \pi^+ \pi^-$ decay. The measured branching fractions are $\mathcal{B}(B^0 \rightarrow K^+ K^-) = (7.80 \pm 1.27 \pm 0.81 \pm 0.21) \times 10^{-8}$ and $\mathcal{B}(B_s^0 \rightarrow \pi^+ \pi^-) = (6.91 \pm 0.54 \pm 0.63 \pm 0.19 \pm 0.40) \times 10^{-7}$. The first uncertainty is statistical, the second is systematic, the third is due to the uncertainty on the $B^0 \rightarrow K^+ \pi^-$ branching fraction used as a normalization. For the B_s^0 mode, the fourth accounts for the uncertainty on the ratio of the probabilities for b quarks to hadronize into B_s^0 and B^0 mesons.

DOI: 10.1103/PhysRevLett.118.081801

The understanding of the dynamics governing the decays of heavy-flavored hadrons is a fundamental ingredient in the search for new particles and new interactions beyond those included in the Standard Model of particle physics (SM). The comparison of theoretical predictions and experimental measurements enables the validity of the SM to be tested up to energy scales well beyond those directly accessible by current particle accelerators. In the last two decades, the development of effective theories significantly improved the accuracy of theoretical predictions for the partial widths of such decays. Several approaches are used to deal with the complexity of quantum chromodynamics (QCD) computations, like QCD factorization (QCDF) [1–3], perturbative QCD (pQCD) [4,5], and soft collinear effective theory (SCET) [6]. Despite the general progress in the field, calculations of decay amplitudes governed by so-called weak annihilation transitions are still affected by large uncertainties. In the SM, the rare decay modes $B^0 \rightarrow K^+ K^-$ and $B_s^0 \rightarrow \pi^+ \pi^-$ (charge conjugate modes are implied throughout) can proceed only through such transitions, whose contributions are expected to be small but could be enhanced through certain rescattering effects [7]. The corresponding Feynman graphs are shown in Fig. 1. Precise knowledge of the branching fractions of these decays is thus needed to improve our understanding of QCD dynamics in the more general sector of two-body b -hadron decays. The $B^0 \rightarrow K^+ K^-$ and $B_s^0 \rightarrow \pi^+ \pi^-$ decays play also a role in

techniques proposed to measure the angle γ of the unitary triangle [8].

While the $B_s^0 \rightarrow \pi^+ \pi^-$ decay has already been observed [9], no evidence exists for the $B^0 \rightarrow K^+ K^-$ decay to date, despite searches performed by the BABAR [10], CDF [11], Belle [12], and LHCb [9] Collaborations. Averages of the measurements of the branching fractions of these two decays are given by the Heavy Flavor Averaging Group (HFAG): $\mathcal{B}(B^0 \rightarrow K^+ K^-) = (0.13^{+0.06}_{-0.05}) \times 10^{-6}$ (corresponding to an upper limit of 0.23×10^{-6} at 95% confidence level) and $\mathcal{B}(B_s^0 \rightarrow \pi^+ \pi^-) = (0.76 \pm 0.13) \times 10^{-6}$ [13]. The results of a new search for the $B^0 \rightarrow K^+ K^-$ decay and an update of the branching fraction measurement of the $B_s^0 \rightarrow \pi^+ \pi^-$ decay are presented in this Letter. The data sample that is analyzed corresponds to integrated luminosities of 1.0 fb⁻¹ at $\sqrt{s} = 7$ TeV and 2.0 fb⁻¹ at $\sqrt{s} = 8$ TeV of pp collision data collected with the LHCb detector in 2011 and 2012, respectively.

The LHCb detector [14,15] is a single-arm forward spectrometer covering the pseudorapidity range $2 < \eta < 5$. The tracking system consists of a silicon-strip vertex detector surrounding the pp interaction region, a large-area silicon-strip detector located upstream of a dipole magnet with a bending power of about 4 Tm, and three stations of silicon-strip detectors and straw drift tubes placed downstream of the magnet. The particle identification (PID) system consists of two ring-imaging Cherenkov

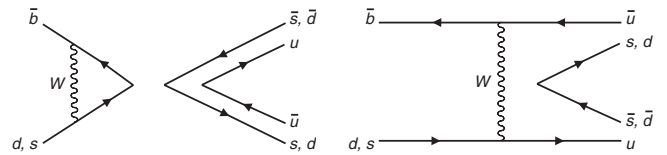


FIG. 1. Dominant Feynman graphs contributing to the $B^0 \rightarrow K^+ K^-$ and $B_s^0 \rightarrow \pi^+ \pi^-$ decay amplitudes: (left) penguin-annihilation and (right) W -exchange topologies.

*Full author list given at the end of the article.

Published by the American Physical Society under the terms of the Creative Commons Attribution 4.0 International license. Further distribution of this work must maintain attribution to the author(s) and the published article's title, journal citation, and DOI.

(RICH) detectors, scintillating-pad and preshower detectors, electromagnetic and hadronic calorimeters, and a set of multiwire proportional chambers alternated with iron absorbers.

Simulated events are used in various steps of the analysis. In the simulation, pp collisions are generated using Pythia [16,17] with a specific LHCb configuration [18]. The interaction of the generated particles with the detector and its response are implemented using the Geant4 toolkit [19], as described in Ref. [20].

The on-line event selection is performed by a trigger [21], which consists of a hardware stage, based on information from the calorimeter and muon systems, followed by a software stage, which applies a full event reconstruction and requires a secondary vertex (SV) with a significant displacement from all primary pp interaction vertices (PVs). At least one charged particle must have high transverse momentum, p_T , and large χ^2_{IP} with respect to all PVs, where χ^2_{IP} is the difference between the χ^2 of the PV fit performed with and without the considered particle. An algorithm based on a boosted decision tree (BDT) multivariate classifier [22,23] is used for the identification of secondary vertices consistent with the decays of b hadrons [24]. To further increase the trigger efficiency, an exclusive selection algorithm for two-body b -hadron decays was put in place, imposing requirements on the following quantities: the quality of the reconstructed tracks, their p_T and impact parameter (IP), the distance of closest approach between the two oppositely charged tracks used to reconstruct the b -hadron candidate, and the p_T , IP and proper decay time of the b -hadron candidate.

The event selection is refined off-line using another BDT classifier and requirements on PID variables. The BDT returns a discriminant variable which is used to classify each b -hadron candidate as either signal or background. With the exception of the b -hadron decay time, the input variables to the BDT classifier are those used in the software trigger, plus the following: the largest p_T and IP of the b -hadron decay products, the χ^2_{IP} of the b -hadron candidate, the χ^2 of the SV fit, and information on the separation of the SV from the PV. In the presence of multiple PVs per event (up to six and with an average of about two in this analysis), the one with the smallest χ^2_{IP} of the b -hadron candidate is considered.

The PID system is used to separate the data into mutually exclusive subsamples corresponding to various hypotheses for the final state, namely, $K^+\pi^-$, pK^- , $p\pi^-$, as well as $\pi^+\pi^-$ and K^+K^- . The calibration of the PID variables is necessary to determine the yields of other two-body b -hadron decays, where one or two particles in the final state are misidentified (cross-feed backgrounds). The efficiencies for a given PID requirement are determined using samples of kaons and pions from the $D^{*+} \rightarrow D^0(\rightarrow K^-\pi^+)\pi^+$ decay chain and protons from $\Lambda \rightarrow p\pi^-$ and $\Lambda_c^+ \rightarrow pK^-\pi^+$ decays. Since the RICH-based PID

information depends on particle momentum, pseudorapidity, and track multiplicity, the efficiencies are determined in bins of these variables. They are then averaged over the momentum and pseudorapidity distributions of the final state particles of two-body b -hadron decays, and over the distribution of track multiplicity in the corresponding events. Uncertainties on the PID efficiencies are due to the finite sizes of the calibration samples and to the binning used to calculate the efficiencies. The size of the latter uncertainty is estimated by the maximum variation when repeating the PID calibration procedure using different binning schemes.

The final selection criteria on the BDT output and PID variables are separately optimized for the $B^0 \rightarrow K^+K^-$ and $B_s^0 \rightarrow \pi^+\pi^-$ decays. The outcome of the optimization consists of two event selections, $S_{K^+K^-}$ and $S_{\pi^+\pi^-}$, aiming at the best sensitivity on the $B^0 \rightarrow K^+K^-$ and $B_s^0 \rightarrow \pi^+\pi^-$ signal yields, respectively. In the two selections, common PID requirements are applied to define the subsamples with final-state mass hypotheses other than K^+K^- and $\pi^+\pi^-$. The optimization procedure is based on pseudoexperiments generating K^+K^- and $\pi^+\pi^-$ invariant mass distributions. Fits to these distributions are performed with a model identical to that used for the generation. The $B_{(s)}^0 \rightarrow K^+K^-$ and $B_{(s)}^0 \rightarrow \pi^+\pi^-$ components are each described by a sum of two Gaussian functions with a common mean to account for mass resolution effects, with parameters determined from data, convolved with a power-law distribution that accounts for final state radiation (FSR) effects. In particular, the $B_s^0 \rightarrow K^+K^-$ mass shape is deformed due to FSR in the region, where the $B^0 \rightarrow K^+K^-$ signal is expected. The power-law distribution is derived from analytical quantum electrodynamics (QED) calculations [25], and the correctness of the model is checked against simulated events generated by Photos [26]. Photos simulates QED-photon emissions in decays by calculating $\mathcal{O}(\alpha)$ radiative corrections for charged particles using a leading-log collinear approximation. Within the approximation, the program calculates the amount of bremsstrahlung in the decay and modifies the final state according to the decay topology. The mass distributions of simulated B candidates, generated with Photos, are well described by fits performed using the mass model developed in this analysis. The fit results are in excellent agreement with the theoretical values of the FSR parameters calculated according to Ref. [25] for each of the decay modes under study.

The background due to the random association of two oppositely charged tracks (combinatorial background) is modeled with an exponential function. The backgrounds due to the partial reconstruction of multibody b -hadron decays are parametrized by means of ARGUS functions [27] convolved with the same resolution function used for the signals. In the case of partially reconstructed $B \rightarrow K^+\pi^-X$ decays, where X stands for one or more missing particles, and the pion is misidentified as a kaon, an incorrect description may alter the determination of the

$B^0 \rightarrow K^+K^-$ signal yield. Hence, the shape of the mass distribution and the size of this contribution to the K^+K^- mass spectrum are determined from data by studying a sample of events selected with tight $K^+\pi^-$ PID requirements and accounting for the known effects of different PID selection criteria on the invariant mass resolution. The shapes of the mass distributions for cross-feed backgrounds are determined by means of a kernel estimation method [28] applied to the invariant mass distributions of simulated two-body b -hadron decays. As the $B^0 \rightarrow K^+\pi^-$ cross feed background contributes to the K^+K^- mass distribution in the $B^0 \rightarrow K^+K^-$ signal mass region, the resulting shape of the mass spectrum is validated with data using again a sample of events selected with tight $K^+\pi^-$ PID requirements. The amounts of cross-feed backgrounds are determined relative to the yields of the $B_s^0 \rightarrow K^+K^-$ and $B^0 \rightarrow \pi^+\pi^-$ decays, scaled by the branching fractions, PID efficiencies, and b -quark hadronization probabilities to form B^0 or B_s^0 mesons [29].

For a given set of BDT and PID selection requirements, pseudoexperiments are generated with yields and model parameters of the backgrounds as determined from data. Signal decays are injected into simulated mass distributions according to different hypotheses for the values of their branching fractions. For each pseudoexperiment, the significance of the signal under study is computed according to Wilks' theorem [30] as $\sqrt{2 \ln(\mathcal{L}_{S+B}/\mathcal{L}_B)}$, where \mathcal{L}_{S+B} and \mathcal{L}_B are the likelihoods of the nominal fit and of a fit where the yield of the signal is fixed to zero, respectively. As the $B^0 \rightarrow K^+K^-$ decay is still not observed and its branching fraction not well constrained, a multidimensional scan is performed over a wide range of branching fraction values, as well as

BDT and PID selection requirements. For each point of the scan, the signal significance is determined. The point corresponding to the smallest branching fraction that can be measured with a significance of 5 standard deviations is determined, and the optimal selection requirements are thus identified. This branching fraction is found to be $\mathcal{B}_{\min} \simeq 6 \times 10^{-8}$. In contrast, the expected yield of $B_s^0 \rightarrow \pi^+\pi^-$ decays is more precisely constrained, and the optimization of the selection requirements is found not to depend on the assumed branching fractions within ± 2 standard deviations from the current world average value [13]. The optimization procedure for $S_{K^+K^-}$ leads to tighter PID and looser BDT requirements with respect to $S_{\pi^+\pi^-}$. This is due to the fact that the random association of two kaons is much less likely than that of two pions, and thus, the correct identification of two kaons provides a more powerful rejection of the combinatorial background with respect to that of two pions. As a consequence, the combinatorial background in the $\pi^+\pi^-$ spectrum is best suppressed by the application of tighter requirements on the BDT output.

After applying the BDT and PID criteria for $S_{K^+K^-}$ or $S_{\pi^+\pi^-}$, the signal yields are determined by means of an extended binned maximum likelihood fit done simultaneously with the exclusive data sets defined by the different mass hypotheses of particles in the final state. The model fitted to the mass distributions is the same as that used in the optimization of the selection. The amount of each cross feed background contribution is determined directly from the fits, taking into account the appropriate PID efficiency factors. The $m_{K^+K^-}$ and $m_{\pi^+\pi^-}$ invariant mass distributions are shown in Fig. 2, with the results of the best fits superimposed. The yields for the two signals are

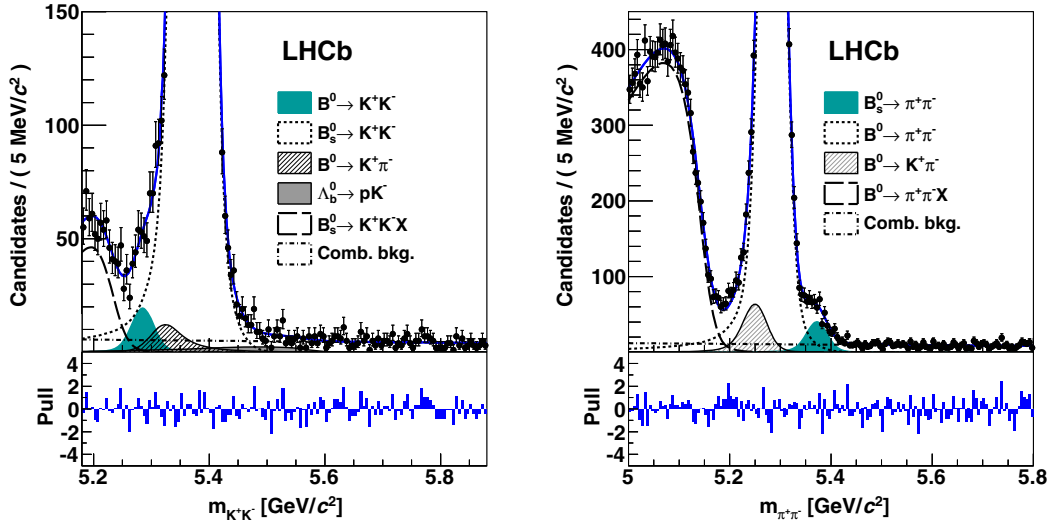


FIG. 2. Distributions of (left) $m_{K^+K^-}$ and (right) $m_{\pi^+\pi^-}$ for candidates passing $S_{K^+K^-}$ and $S_{\pi^+\pi^-}$, respectively. The continuous (blue) curves represent the results of the best fits to the data points. The most relevant contributions to the invariant mass spectra are shown as indicated in the legends. The vertical scales are chosen to magnify the relevant signal regions. The bin-by-bin differences between the fits and the data, in units of standard deviations, are also shown.

TABLE I. Systematic uncertainties on the yields for the $B^0 \rightarrow K^+K^-$ and $B_s^0 \rightarrow \pi^+\pi^-$ decays.

Systematic uncertainty	$N(B^0 \rightarrow K^+K^-)$	$N(B_s^0 \rightarrow \pi^+\pi^-)$
Signal mass shape	11.8	6.3
Combinatorial mass shape	5.5	2.6
Partially reco. mass shape	1.3	23.1
PID efficiencies	3.4	2.5
Sum in quadrature	13.5	24.2

$N(B^0 \rightarrow K^+K^-) = 201 \pm 33 \pm 14$ and $N(B_s^0 \rightarrow \pi^+\pi^-) = 455 \pm 35 \pm 24$, where the first uncertainty is statistical and the second is systematic. The systematic uncertainties are related to the choice of the model used to parametrize the invariant mass shapes of signal and background components and to the knowledge of the PID efficiencies used to determine the amount of cross-feed backgrounds. The results of the best fits are used to generate pseudoexperiments, and then fits with alternative models are applied to the mass distributions. By studying the distributions of the difference between the signal yields determined from the nominal fit and those performed with alternative models, systematic uncertainties are determined. Such alternative models are considered for signal, combinatorial background, background from partially reconstructed b -hadron decays, and cross feed background mass models. The systematic uncertainty due to PID efficiencies is also assessed by generating pseudoexperiments and fitting the nominal model to the output mass distributions, using PID efficiencies randomly varied in each pseudoexperiment according to their estimated uncertainties. The standard deviation of the distribution of the yields determined in each set of pseudoexperiments is taken as a systematic uncertainty. The contributions of the various systematic uncertainties are reported in Table I. The systematic uncertainties associated to the knowledge of the cross feed background mass shapes are found to be negligible and are not reported. The total systematic uncertainties are obtained by summing all contributions in quadrature.

The significance of the $B^0 \rightarrow K^+K^-$ signal with respect to the null hypothesis is determined by means of a profile likelihood ratio. To account for systematic uncertainties, the likelihood function is convolved with a Gaussian function with width equal to the systematic uncertainty. The log-likelihood ratio as a function of the $B^0 \rightarrow K^+K^-$ signal yield is shown in Fig. 3. The statistical significance is found to be 6.3 standard deviations, reduced to 5.8 when considering systematic uncertainties.

The branching fractions of $B^0 \rightarrow K^+K^-$ and $B_s^0 \rightarrow \pi^+\pi^-$ decays are determined relative to the $B^0 \rightarrow K^+\pi^-$ branching fraction, according to the following equation:

$$\frac{f_x \mathcal{B}(B_x^0 \rightarrow h^+h^-)}{f_d \mathcal{B}(B^0 \rightarrow K^+\pi^-)} = \frac{N(B_x^0 \rightarrow h^+h^-) \varepsilon(B^0 \rightarrow K^+\pi^-)}{N(B^0 \rightarrow K^+\pi^-) \varepsilon(B_x^0 \rightarrow h^+h^-)},$$

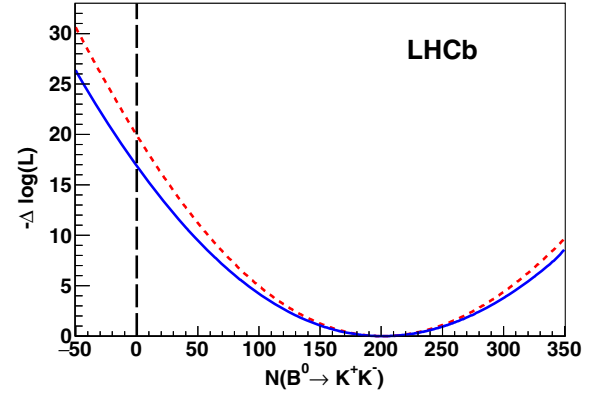


FIG. 3. Log-likelihood ratio as a function of the $B^0 \rightarrow K^+K^-$ signal yield. The dashed (red) and continuous (blue) curves correspond to the exclusion and to the inclusion of systematic uncertainties, respectively.

where f_x is the probability for a b quark to hadronize into a B_x^0 meson ($x = d, s$), N and ε are the yield and the efficiency for the given decay mode, respectively, and h stands for K or π . The yields of the $B^0 \rightarrow K^+\pi^-$ decay in the subsamples selected with $K^+\pi^-$ PID requirements are determined from the fits, and their values are $N(B^0 \rightarrow K^+\pi^-) = 105010 \pm 431 \pm 988$ and $N(B^0 \rightarrow K^+\pi^-) = 71304 \pm 312 \pm 609$, when applying the BDT requirements of $S_{K^+K^-}$ and $S_{\pi^+\pi^-}$, respectively. Trigger and reconstruction efficiencies are determined from simulation and corrected using information from data. For the $B_s^0 \rightarrow \pi^+\pi^-$ decay, the sizeable value of the decay width difference between the long- and short-lived components of the B_s^0 -meson system is taken into account. The $B_s^0 \rightarrow \pi^+\pi^-$ lifetime is assumed to be that of the short-lived component, as expected in presence of small CP violation. The final ratios of efficiencies are found to be 2.08 ± 0.16 and 1.43 ± 0.10 for the $B^0 \rightarrow K^+K^-$ and $B_s^0 \rightarrow \pi^+\pi^-$ decays, respectively. The dominant contributions to the uncertainties on these ratios are due to the PID calibration and to the knowledge of the trigger efficiencies. The following results are then obtained:

$$\frac{\mathcal{B}(B^0 \rightarrow K^+K^-)}{\mathcal{B}(B^0 \rightarrow K^+\pi^-)} = (3.98 \pm 0.65 \pm 0.42) \times 10^{-3},$$

$$\frac{f_s \mathcal{B}(B_s^0 \rightarrow \pi^+\pi^-)}{f_d \mathcal{B}(B^0 \rightarrow K^+\pi^-)} = (9.15 \pm 0.71 \pm 0.83) \times 10^{-3},$$

where the first uncertainty is statistical and the second systematic. Using the HFAG average $\mathcal{B}(B^0 \rightarrow K^+\pi^-) = (19.57^{+0.53}_{-0.52}) \times 10^{-6}$ [13], and $f_s/f_d = 0.259 \pm 0.015$ from Ref. [29], the following branching fractions are obtained:

$$\mathcal{B}(B^0 \rightarrow K^+K^-) = (7.80 \pm 1.27 \pm 0.81 \pm 0.21) \times 10^{-8},$$

$$\mathcal{B}(B_s^0 \rightarrow \pi^+\pi^-) = (6.91 \pm 0.54 \pm 0.63 \pm 0.19 \pm 0.40) \times 10^{-7},$$

where the first uncertainty is statistical, the second systematic, and the third and fourth are due to the knowledge of $\mathcal{B}(B^0 \rightarrow K^+\pi^-)$ and of f_s/f_d , respectively.

Various theoretical predictions of the branching fractions of $B^0 \rightarrow K^+K^-$ and $B_s^0 \rightarrow \pi^+\pi^-$ decays are available in the literature [2–5,7,31–35]. The pQCD estimations in Ref. [5] are in agreement within uncertainties with the present results. The QCDF prediction of $\mathcal{B}(B^0 \rightarrow K^+K^-)$ in Ref. [2] agrees well with these results, but that of $\mathcal{B}(B_s^0 \rightarrow \pi^+\pi^-)$ is significantly smaller than the measurement. In Ref. [34], the unexpectedly large value of $\mathcal{B}(B_s^0 \rightarrow \pi^+\pi^-)$ caused the traditional QCDF treatment for annihilation parameters to be revisited.

In summary, this Letter reports the most precise measurements of the branching fractions for the $B^0 \rightarrow K^+K^-$ and $B_s^0 \rightarrow \pi^+\pi^-$ decay modes to date. These are in good agreement with and supersede those reported in Ref. [9], which were the best results available prior to the present analysis. The $B^0 \rightarrow K^+K^-$ decay is the rarest fully hadronic B -meson decay ever observed.

We express our gratitude to our colleagues in the CERN accelerator departments for the excellent performance of the LHC. We thank the technical and administrative staff at the LHCb institutes. We acknowledge support from CERN and from the national agencies: CAPES, CNPq, FAPERJ, and FINEP (Brazil); NSFC (China); CNRS/IN2P3 (France); BMBF, DFG, and MPG (Germany); INFN (Italy); FOM and NWO (Netherlands); MNiSW and NCN (Poland); MEN/IFA (Romania); MinES and FASO (Russia); MinECo (Spain); SNSF and SER (Switzerland); NASU (Ukraine); STFC (United Kingdom); NSF (USA). We acknowledge the computing resources that are provided by CERN, IN2P3 (France), KIT and DESY (Germany), INFN (Italy), SURF (Netherlands), PIC (Spain), GridPP (United Kingdom), RRCKI and Yandex LLC (Russia), CSCS (Switzerland), IFIN-HH (Romania), CBPF (Brazil), PL-GRID (Poland), and OSC (USA). We are indebted to the communities behind the multiple open source software packages on which we depend. Individual groups or members have received support from AvH Foundation (Germany); EPLANET, Marie Skłodowska-Curie Actions and ERC (European Union); Conseil Général de Haute-Savoie, Labex ENIGMASS and OCEVU, Région Auvergne (France); RFBR and Yandex LLC (Russia); GVA, XuntaGal, and GENCAT (Spain); Herchel Smith Fund, The Royal Society, Royal Commission for the Exhibition of 1851, and the Leverhulme Trust (United Kingdom).

-
- [1] M. Beneke and M. Neubert, *Nucl. Phys.* **B675**, 333 (2003).
 [2] H.-Y. Cheng and C.-K. Chua, *Phys. Rev. D* **80**, 114026 (2009).

- [3] H.-Y. Cheng and C.-K. Chua, *Phys. Rev. D* **80**, 114008 (2009).
 [4] A. Ali, G. Kramer, Y. Li, C.-D. Lu, Y.-L. Shen, W. Wang, and Y.-M. Wang, *Phys. Rev. D* **76**, 074018 (2007).
 [5] Z.-J. Xiao, W.-F. Wang, and Y.-Y. Fan, *Phys. Rev. D* **85**, 094003 (2012).
 [6] C. W. Bauer, D. Pirjol, I. Z. Rothstein, and I. W. Stewart, *Phys. Rev. D* **70**, 054015 (2004).
 [7] M. Gronau, D. London, and J. L. Rosner, *Phys. Rev. D* **87**, 036008 (2013).
 [8] R. Fleischer, *Phys. Lett. B* **459**, 306 (1999).
 [9] R. Aaij *et al.* (LHCb Collaboration), *J. High Energy Phys.* **10** (2012) 037.
 [10] B. Aubert *et al.* (BABAR Collaboration), *Phys. Rev. D* **75**, 012008 (2007).
 [11] T. Aaltonen *et al.* (CDF Collaboration), *Phys. Rev. Lett.* **108**, 211803 (2012).
 [12] Y. T. Duh *et al.* (Belle Collaboration), *Phys. Rev. D* **87**, 031103 (2013).
 [13] Y. Amhis *et al.* (Heavy Flavor Averaging Group), updated results and plots available at <http://www.slac.stanford.edu/xorg/hfag/>, arXiv:1412.7515.
 [14] A. A. Alves Jr. *et al.* (LHCb Collaboration), *J. Instrum.* **3**, S08005 (2008).
 [15] R. Aaij *et al.* (LHCb Collaboration), *Int. J. Mod. Phys. A* **30**, 1530022 (2015).
 [16] T. Sjöstrand, S. Mrenna, and P. Skands, *J. High Energy Phys.* **05** (2006) 026.
 [17] T. Sjöstrand, S. Mrenna, and P. Skands, *Comput. Phys. Commun.* **178**, 852 (2008).
 [18] I. Belyaev *et al.*, *J. Phys. Conf. Ser.* **331**, 032047 (2011).
 [19] J. Allison, K. Amako, J. Apostolakis, H. Araujo, P. Dubois *et al.* (GEANT4 Collaboration), *IEEE Trans. Nucl. Sci.* **53**, 270 (2006); S. Agostinelli *et al.* (GEANT4 Collaboration), *Nucl. Instrum. Methods Phys. Res., Sect. A* **506**, 250 (2003).
 [20] M. Clemencic, G. Corti, S. Easo, C. R. Jones, S. Miglioranza, M. Pappagallo, and P. Robbe, *J. Phys. Conf. Ser.* **331**, 032023 (2011).
 [21] R. Aaij *et al.*, *J. Instrum.* **8**, P04022 (2013).
 [22] L. Breiman, J. H. Friedman, R. A. Olshen, and C. J. Stone, *Classification and Regression Trees* (Wadsworth International Group, Belmont, 1984).
 [23] B. P. Roe, H.-J. Yang, J. Zhu, Y. Liu, I. Stancu, and G. McGregor, *Nucl. Instrum. Methods Phys. Res., Sect. A* **543**, 577 (2005).
 [24] V. V. Gligorov and M. Williams, *J. Instrum.* **8**, P02013 (2013).
 [25] E. Baracchini and G. Isidori, *Phys. Lett. B* **633**, 309 (2006).
 [26] P. Golonka and Z. Was, *Eur. Phys. J. C* **45**, 97 (2006).
 [27] H. Albrecht *et al.* (ARGUS Collaboration), *Phys. Lett. B* **340**, 217 (1994).
 [28] K. S. Cranmer, *Comput. Phys. Commun.* **136**, 198 (2001).
 [29] R. Aaij *et al.* (LHCb Collaboration), *J. High Energy Phys.* **04** (2013) 001, f_s/f_d value updated in LHCb-CONF-2013-011.
 [30] S. S. Wilks, *Ann. Math. Stat.* **9**, 60 (1938).

- [31] C.-D. Lu, Y.-L. Shen, and W. Wang, *Phys. Rev. D* **73**, 034005 (2006).
 [32] K. Wang and G. Zhu, *Phys. Rev. D* **88**, 014043 (2013).
 [33] Q. Chang, J. Sun, Y. Yang, and X. Li, *Phys. Rev. D* **90**, 054019 (2014).
 [34] Q. Chang, J. Sun, Y. Yang, and X. Li, *Phys. Lett. B* **740**, 56 (2015).
 [35] Y. Li, W.-L. Wang, D.-S. Du, Z.-H. Li, and H.-X. Xu, *Eur. Phys. J. C* **75**, 328 (2015).

R. Aaij,⁴⁰ B. Adeva,³⁹ M. Adinolfi,⁴⁸ Z. Ajaltouni,⁵ S. Akar,⁶ J. Albrecht,¹⁰ F. Alessio,⁴⁰ M. Alexander,⁵³ S. Ali,⁴³ G. Alkhazov,³¹ P. Alvarez Cartelle,⁵⁵ A. A. Alves Jr.,⁵⁹ S. Amato,² S. Amerio,²³ Y. Amhis,⁷ L. An,⁴¹ L. Anderlini,¹⁸ G. Andreassi,⁴¹ M. Andreotti,^{17,g} J. E. Andrews,⁶⁰ R. B. Appleby,⁵⁶ F. Archilli,⁴³ P. d'Argent,¹² J. Arnau Romeu,⁶ A. Artamonov,³⁷ M. Artuso,⁶¹ E. Aslanides,⁶ G. Auriemma,²⁶ M. Baalouch,⁵ I. Babuschkin,⁵⁶ S. Bachmann,¹² J. J. Back,⁵⁰ A. Badalov,³⁸ C. Baesso,⁶² S. Baker,⁵⁵ W. Baldini,¹⁷ R. J. Barlow,⁵⁶ C. Barschel,⁴⁰ S. Barsuk,⁷ W. Barter,⁴⁰ M. Baszczyk,²⁷ V. Batozskaya,²⁹ B. Batsukh,⁶¹ V. Battista,⁴¹ A. Bay,⁴¹ L. Beaucourt,⁴ J. Beddow,⁵³ F. Bedeschi,²⁴ I. Bediaga,¹ L. J. Bel,⁴³ V. Bellee,⁴¹ N. Belloli,^{21,i} K. Belous,³⁷ I. Belyaev,³² E. Ben-Haim,⁸ G. Bencivenni,¹⁹ S. Benson,⁴³ J. Benton,⁴⁸ A. Berezhnoy,³³ R. Bernet,⁴² A. Bertolin,²³ F. Betti,¹⁵ M.-O. Bettler,⁴⁰ M. van Beuzekom,⁴³ I. Bezshyiko,⁴² S. Bifani,⁴⁷ P. Billoir,⁸ T. Bird,⁵⁶ A. Birnkraut,¹⁰ A. Bitadze,⁵⁶ A. Bizzeti,^{18,u} T. Blake,⁵⁰ F. Blanc,⁴¹ J. Blouw,^{11,†} S. Blusk,⁶¹ V. Bocci,²⁶ T. Boettcher,⁵⁸ A. Bondar,^{36,w} N. Bondar,^{31,40} W. Bonivento,¹⁶ A. Borgheresi,^{21,i} S. Borghi,⁵⁶ M. Borisyak,³⁵ M. Borsato,³⁹ F. Bossu,⁷ M. Boudir,⁹ T. J. V. Bowcock,⁵⁴ E. Bowen,⁴² C. Bozzi,^{17,40} S. Braun,¹² M. Britsch,¹² T. Britton,⁶¹ J. Brodzicka,⁵⁶ E. Buchanan,⁴⁸ C. Burr,⁵⁶ A. Bursche,² J. Buytaert,⁴⁰ S. Cadeddu,¹⁶ R. Calabrese,^{17,g} M. Calvi,^{21,i} M. Calvo Gomez,^{38,m} A. Camboni,³⁸ P. Campana,¹⁹ D. Campora Perez,⁴⁰ D. H. Campora Perez,⁴⁰ L. Capriotti,⁵⁶ A. Carbone,^{15,e} G. Carboni,^{25,j} R. Cardinale,^{20,h} A. Cardini,¹⁶ P. Carniti,^{21,i} L. Carson,⁵² K. Carvalho Akiba,² G. Casse,⁵⁴ L. Cassina,^{21,i} L. Castillo Garcia,⁴¹ M. Cattaneo,⁴⁰ Ch. Cauet,¹⁰ G. Cavallero,²⁰ R. Cenci,^{24,t} M. Charles,⁸ Ph. Charpentier,⁴⁰ G. Chatzikonstantinidis,⁴⁷ M. Chefdeville,⁴ S. Chen,⁵⁶ S.-F. Cheung,⁵⁷ V. Chobanova,³⁹ M. Chrzasczcz,^{42,27} X. Cid Vidal,³⁹ G. Ciezarek,⁴³ P. E. L. Clarke,⁵² M. Clemencic,⁴⁰ H. V. Cliff,⁴⁹ J. Closier,⁴⁰ V. Coco,⁵⁹ J. Cogan,⁶ E. Cogneras,⁵ V. Cogoni,^{16,40,f} L. Cojocariu,³⁰ G. Collazuol,^{23,o} P. Collins,⁴⁰ A. Comerma-Montells,¹² A. Contu,⁴⁰ A. Cook,⁴⁸ G. Coombs,⁴⁰ S. Coquereau,³⁸ G. Corti,⁴⁰ M. Corvo,^{17,g} C. M. Costa Sobral,⁵⁰ B. Couturier,⁴⁰ G. A. Cowan,⁵² D. C. Craik,⁵² A. Crocombe,⁵⁰ M. Cruz Torres,⁶² S. Cunliffe,⁵⁵ R. Currie,⁵⁵ C. D'Ambrosio,⁴⁰ F. Da Cunha Marinho,² E. Dall'Occo,⁴³ J. Dalseno,⁴⁸ P. N. Y. David,⁴³ A. Davis,⁵⁹ O. De Aguiar Francisco,² K. De Bruyn,⁶ S. De Capua,⁵⁶ M. De Cian,¹² J. M. De Miranda,¹ L. De Paula,² M. De Serio,^{14,d} P. De Simone,¹⁹ C. T. Dean,⁵³ D. Decamp,⁴ M. Deckenhoff,¹⁰ L. Del Buono,⁸ M. Demmer,¹⁰ D. Derkach,³⁵ O. Deschamps,⁵ F. Dettori,⁴⁰ B. Dey,²² A. Di Canto,⁴⁰ H. Dijkstra,⁴⁰ F. Dordei,⁴⁰ M. Dorigo,⁴¹ A. Dosil Suárez,³⁹ A. Dovbnya,⁴⁵ K. Dreimanis,⁵⁴ L. Dufour,⁴³ G. Dujany,⁵⁶ K. Dungs,⁴⁰ P. Durante,⁴⁰ R. Dzhelezhad, A. Dziurda,⁴⁰ A. Dzyuba,³¹ N. Deléage,⁴ S. Easo,⁵¹ M. Ebert,⁵² U. Egede,⁵⁵ V. Egorychev,³² S. Eidelman,^{36,w} S. Eisenhardt,⁵² U. Eitschberger,¹⁰ R. Ekelhof,¹⁰ L. Eklund,⁵³ Ch. Elsasser,⁴² S. Ely,⁶¹ S. Esen,¹² H. M. Evans,⁴⁹ T. Evans,⁵⁷ A. Falabella,¹⁵ N. Farley,⁴⁷ S. Farry,⁵⁴ R. Fay,⁵⁴ D. Fazzini,^{21,i} D. Ferguson,⁵² V. Fernandez Albor,³⁹ A. Fernandez Prieto,³⁹ F. Ferrari,^{15,40} F. Ferreira Rodrigues,¹ M. Ferro-Luzzi,⁴⁰ S. Filippov,³⁴ R. A. Fini,¹⁴ M. Fiore,^{17,g} M. Fiorini,^{17,g} M. Firlej,²⁸ C. Fitzpatrick,⁴¹ T. Fiutowski,²⁸ F. Fleuret,^{7,b} K. Fohl,⁴⁰ M. Fontana,^{16,40} F. Fontanelli,^{20,h} D. C. Forshaw,⁶¹ R. Forty,⁴⁰ V. Franco Lima,⁵⁴ M. Frank,⁴⁰ C. Frei,⁴⁰ J. Fu,^{22,q} E. Furfaro,^{25,j} C. Färber,⁴⁰ A. Gallas Torreira,³⁹ D. Galli,^{15,e} S. Gallorini,²³ S. Gambetta,⁵² M. Gandelman,² P. Gandini,⁵⁷ Y. Gao,³ L. M. Garcia Martin,⁶⁸ J. García Pardiñas,³⁹ J. Garra Tico,⁴⁹ L. Garrido,³⁸ P. J. Garsed,⁴⁹ D. Gascon,³⁸ C. Gaspar,⁴⁰ L. Gavardi,¹⁰ G. Gazzoni,⁵ D. Gerick,¹² E. Gersabeck,¹² M. Gersabeck,⁵⁶ T. Gershon,⁵⁰ Ph. Ghez,⁴ S. Giani,⁴¹ V. Gibson,⁴⁹ O. G. Girard,⁴¹ L. Giubega,³⁰ K. Gizdov,⁵² V. V. Gligorov,⁸ D. Golubkov,³² A. Golutvin,^{55,40} A. Gomes,^{1,a} I. V. Gorelov,³³ C. Gotti,^{21,i} M. Grabalosa Gándara,⁵ R. Graciani Diaz,³⁸ L. A. Granado Cardoso,⁴⁰ E. Graugés,³⁸ E. Graverini,⁴² G. Graziani,¹⁸ A. Greco,³⁰ P. Griffith,⁴⁷ L. Grillo,^{21,40,i} B. R. Gruber Cazon,⁵⁷ O. Grünberg,⁶⁶ E. Gushchin,³⁴ Yu. Guz,³⁷ T. Gys,⁴⁰ C. Göbel,⁶² T. Hadavizadeh,⁵⁷ C. Hadjivasiliou,⁵ G. Haefeli,⁴¹ C. Haen,⁴⁰ S. C. Haines,⁴⁹ S. Hall,⁵⁵ B. Hamilton,⁶⁰ X. Han,¹² S. Hansmann-Menzemer,¹² N. Harnew,⁵⁷ S. T. Harnew,⁴⁸ J. Harrison,⁵⁶ M. Hatch,⁴⁰ J. He,⁶³ T. Head,⁴¹ A. Heister,⁹ K. Hennessy,⁵⁴ P. Henrard,⁵ L. Henry,⁸ J. A. Hernando Morata,³⁹ E. van Herwijnen,⁴⁰ M. Heß,⁶⁶ A. Hicheur,² D. Hill,⁵⁷ C. Hombach,⁵⁶ H. Hopchev,⁴¹ W. Hulsbergen,⁴³ T. Humair,⁵⁵ M. Hushchyn,³⁵ N. Hussain,⁵⁷ D. Hutchcroft,⁵⁴ M. Idzik,²⁸ P. Ilten,⁵⁸ R. Jacobsson,⁴⁰ A. Jaeger,¹² J. Jalocha,⁵⁷ E. Jans,⁴³ A. Jawahery,⁶⁰ F. Jiang,³ M. John,⁵⁷ D. Johnson,⁴⁰ C. R. Jones,⁴⁹ C. Joram,⁴⁰ B. Jost,⁴⁰ N. Jurik,⁶¹ S. Kandybei,⁴⁵ W. Kanso,⁶ M. Karacson,⁴⁰ J. M. Kariuki,⁴⁸ S. Karodia,⁵³

M. Kecke,¹² M. Kelsey,⁶¹ I. R. Kenyon,⁴⁷ M. Kenzie,⁴⁹ T. Ketel,⁴⁴ E. Khairullin,³⁵ B. Khanji,^{21,40,i} C. Khurewathanakul,⁴¹ T. Kim,⁹ S. Klaver,⁵⁶ K. Klimaszewski,²⁹ S. Koliiev,⁴⁶ M. Kolpin,¹² I. Komarov,⁴¹ R. F. Koopman,⁴⁴ P. Koppenburg,⁴³ A. Kosmyntseva,³² A. Kozachuk,³³ M. Kozeiha,⁵ L. Kravchuk,³⁴ K. Kreplin,¹² M. Kreps,⁵⁰ P. Krokovny,^{36,w} F. Kruse,¹⁰ W. Krzemien,²⁹ W. Kucewicz,^{27,l} M. Kucharczyk,²⁷ V. Kudryavtsev,^{36,w} A. K. Kuonen,⁴¹ K. Kurek,²⁹ T. Kvaratskheliya,^{32,40} D. Lacarrere,⁴⁰ G. Lafferty,⁵⁶ A. Lai,¹⁶ D. Lambert,⁵² G. Lanfranchi,¹⁹ C. Langenbruch,⁹ T. Latham,⁵⁰ C. Lazzeroni,⁴⁷ R. Le Gac,⁶ J. van Leerdam,⁴³ J.-P. Lees,⁴ A. Leflat,^{33,40} J. Lefrançois,⁷ R. Lefèvre,⁵ F. Lemaitre,⁴⁰ E. Lemos Cid,³⁹ O. Leroy,⁶ T. Lesiak,²⁷ B. Leverington,¹² Y. Li,⁷ T. Likhomanenko,^{35,67} R. Lindner,⁴⁰ C. Linn,⁴⁰ F. Lionetto,⁴² B. Liu,¹⁶ X. Liu,³ D. Loh,⁵⁰ I. Longstaff,⁵³ J. H. Lopes,² D. Lucchesi,^{23,o} M. Lucio Martinez,³⁹ H. Luo,⁵² A. Lupato,²³ E. Luppi,^{17,g} O. Lupton,⁵⁷ A. Lusiani,²⁴ X. Lyu,⁶³ F. Machefert,⁷ F. Maciuc,³⁰ O. Maev,³¹ K. Maguire,⁵⁶ S. Malde,⁵⁷ A. Malinin,⁶⁷ T. Maltsev,³⁶ G. Manca,⁷ G. Mancinelli,⁶ P. Manning,⁶¹ J. Maratas,^{5,v} J. F. Marchand,⁴ U. Marconi,¹⁵ C. Marin Benito,³⁸ P. Marino,^{24,t} J. Marks,¹² G. Martellotti,²⁶ M. Martin,⁶ M. Martinelli,⁴¹ D. Martinez Santos,³⁹ F. Martinez Vidal,⁶⁸ D. Martins Tostes,² L. M. Massacrier,⁷ A. Massafferri,¹ R. Matev,⁴⁰ A. Mathad,⁵⁰ Z. Mathe,⁴⁰ C. Matteuzzi,²¹ A. Mauri,⁴² B. Maurin,⁴¹ A. Mazurov,⁴⁷ M. McCann,⁵⁵ J. McCarthy,⁴⁷ A. McNab,⁵⁶ R. McNulty,¹³ B. Meadows,⁵⁹ F. Meier,¹⁰ M. Meissner,¹² D. Melnychuk,²⁹ M. Merk,⁴³ A. Merli,^{22,q} E. Michielin,²³ D. A. Milanes,⁶⁵ M.-N. Minard,⁴ D. S. Mitzel,¹² A. Mogini,⁸ J. Molina Rodriguez,⁶² I. A. Monroy,⁶⁵ S. Monteil,⁵ M. Morandin,²³ P. Morawski,²⁸ A. Mordà,⁶ M. J. Morello,^{24,t} J. Moron,²⁸ A. B. Morris,⁵² R. Mountain,⁶¹ F. Muheim,⁵² M. Mulder,⁴³ M. Mussini,¹⁵ D. Müller,⁵⁶ J. Müller,¹⁰ K. Müller,⁴² V. Müller,¹⁰ P. Naik,⁴⁸ T. Nakada,⁴¹ R. Nandakumar,⁵¹ A. Nandi,⁵⁷ I. Nasteva,² M. Needham,⁵² N. Neri,²² S. Neubert,¹² N. Neufeld,⁴⁰ M. Neuner,¹² A. D. Nguyen,⁴¹ C. Nguyen-Mau,^{41,n} S. Nieswand,⁹ R. Niet,¹⁰ N. Nikitin,³³ T. Nikodem,¹² A. Novoselov,³⁷ D. P. O'Hanlon,⁵⁰ A. Oblakowska-Mucha,²⁸ V. Obraztsov,³⁷ S. Ogilvy,¹⁹ R. Oldeman,⁴⁹ C. J. G. Onderwater,⁶⁹ J. M. Otalora Goicochea,² A. Otto,⁴⁰ P. Owen,⁴² A. Oyanguren,⁶⁸ P. R. Pais,⁴¹ A. Palano,^{14,d} F. Palombo,^{22,q} M. Palutan,¹⁹ J. Panman,⁴⁰ A. Papanestis,⁵¹ M. Pappagallo,^{14,d} L. L. Pappalardo,^{17,g} W. Parker,⁶⁰ C. Parkes,⁵⁶ G. Passaleva,¹⁸ A. Pastore,^{14,d} G. D. Patel,⁵⁴ M. Patel,⁵⁵ C. Patrignani,^{15,e} A. Pearce,^{56,51} A. Pellegrino,⁴³ G. Penso,²⁶ M. Pepe Altarelli,⁴⁰ S. Perazzini,⁴⁰ P. Perret,⁵ L. Pescatore,⁴⁷ K. Petridis,⁴⁸ A. Petrolini,^{20,h} A. Petrov,⁶⁷ M. Petruzzo,^{22,q} E. Picatoste Olloqui,³⁸ B. Pietrzyk,⁴ M. Pikies,²⁷ D. Pinci,²⁶ A. Pistone,²⁰ A. Piucci,¹² S. Playfer,⁵² M. Plo Casasus,³⁹ T. Poikela,⁴⁰ F. Polci,⁸ A. Poluektov,^{50,36} I. Polyakov,⁶¹ E. Polcarpo,² G. J. Pomery,⁴⁸ A. Popov,³⁷ D. Popov,^{11,40} B. Popovici,³⁰ S. Poslavskii,³⁷ C. Potterat,² E. Price,⁴⁸ J. D. Price,⁵⁴ J. Prisciandaro,³⁹ A. Pritchard,⁵⁴ C. Prouve,⁴⁸ V. Pugatch,⁴⁶ A. Puig Navarro,⁴¹ G. Punzi,^{24,p} W. Qian,⁵⁷ R. Quagliani,^{7,48} B. Rachwal,²⁷ J. H. Rademacker,⁴⁸ M. Rama,²⁴ M. Ramos Pernas,³⁹ M. S. Rangel,² I. Raniuk,⁴⁵ G. Raven,⁴⁴ F. Redi,⁵⁵ S. Reichert,¹⁰ A. C. dos Reis,¹ C. Remon Alepuz,⁶⁸ V. Renaudin,⁷ S. Ricciardi,⁵¹ S. Richards,⁴⁸ M. Rihl,⁴⁰ K. Rinnert,⁵⁴ V. Rives Molina,³⁸ P. Robbe,^{7,40} A. B. Rodrigues,¹ E. Rodrigues,⁵⁹ J. A. Rodriguez Lopez,⁶⁵ P. Rodriguez Perez,^{56,t} A. Rogozhnikov,³⁵ S. Roiser,⁴⁰ A. Rollings,⁵⁷ V. Romanovskiy,³⁷ A. Romero Vidal,³⁹ J. W. Ronayne,¹³ M. Rotondo,¹⁹ M. S. Rudolph,⁶¹ T. Ruf,⁴⁰ P. Ruiz Valls,⁶⁸ J. J. Saborido Silva,³⁹ E. Sadykhov,³² N. Sagidova,³¹ B. Saitta,^{16,f} V. Salustino Guimaraes,² C. Sanchez Mayordomo,⁶⁸ B. Sanmartin Sedes,³⁹ R. Santacesaria,²⁶ C. Santamarina Rios,³⁹ M. Santimaria,¹⁹ E. Santovetti,^{25,j} A. Sarti,^{19,k} C. Satriano,^{26,s} A. Satta,²⁵ D. M. Saunders,⁴⁸ D. Savrina,^{32,33} S. Schael,⁹ M. Schellenberg,¹⁰ M. Schiller,⁴⁰ H. Schindler,⁴⁰ M. Schlupp,¹⁰ M. Schmelling,¹¹ T. Schmelzer,¹⁰ B. Schmidt,⁴⁰ O. Schneider,⁴¹ A. Schopper,⁴⁰ K. Schubert,¹⁰ M. Schubiger,⁴¹ M.-H. Schune,⁷ R. Schwemmer,⁴⁰ B. Sciascia,¹⁹ A. Sciubba,^{26,k} A. Semennikov,³² A. Sergi,⁴⁷ N. Serra,⁴² J. Serrano,⁶ L. Sestini,²³ P. Seyfert,²¹ M. Shapkin,³⁷ I. Shapoval,⁴⁵ Y. Shcheglov,³¹ T. Shears,⁵⁴ L. Shekhtman,^{36,w} V. Shevchenko,⁶⁷ A. Shires,¹⁰ B. G. Siddi,^{17,40} R. Silva Coutinho,⁴² L. Silva de Oliveira,² G. Simi,^{23,o} S. Simone,^{14,d} M. Sirendi,⁴⁹ N. Skidmore,⁴⁸ T. Skwarnicki,⁶¹ E. Smith,⁵⁵ I. T. Smith,⁵² J. Smith,⁴⁹ M. Smith,⁵⁵ H. Snok,⁴³ M. D. Sokoloff,⁵⁹ F. J. P. Soler,⁵³ B. Souza De Paula,² B. Spaan,¹⁰ P. Spradlin,⁵³ S. Sridharan,⁴⁰ F. Stagni,⁴⁰ M. Stahl,¹² S. Stahl,⁴⁰ P. Stefkova,⁴¹ S. Stefkova,⁵⁵ O. Steinkamp,⁴² S. Stemmler,¹² O. Stenyakin,³⁷ S. Stevenson,⁵⁷ S. Stoica,³⁰ S. Stone,⁶¹ B. Storaci,⁴² S. Stracka,^{24,p} M. Straticiuc,³⁰ U. Straumann,⁴² L. Sun,⁵⁹ W. Sutcliffe,⁵⁵ K. Swientek,²⁸ V. Syropoulos,⁴⁴ M. Szczekowski,²⁹ T. Szumlak,²⁸ S. T'Jampens,⁴ A. Tayduganov,⁶ T. Tekampe,⁶ M. Teklishyn,¹⁰ G. Tellarini,⁷ F. Teubert,^{17,g} E. Thomas,⁴⁰ J. van Tilburg,⁴⁰ M. J. Tilley,⁴³ V. Tisserand,⁵⁵ M. Tobin,⁴¹ S. Tolk,⁴⁹ L. Tomassetti,^{17,g} D. Tonelli,⁴⁰ S. Topp-Joergensen,⁵⁷ F. Toriello,⁶¹ E. Tournefier,⁴ S. Tourneur,⁴¹ K. Trabelsi,⁴¹ M. Traill,⁵³ M. T. Tran,⁴¹ M. Tresch,⁴² A. Trisovic,⁴⁰ A. Tsaregorodtsev,⁶ P. Tsopelas,⁴³ A. Tully,⁴⁹ N. Tuning,⁴³ A. Ukleja,²⁹ A. Ustyuzhanin,³⁵ U. Uwer,¹² C. Vacca,^{16,f} V. Vagnoni,^{15,40} A. Valassi,⁴⁰ S. Valat,⁴⁰ G. Valenti,¹⁵ A. Vallier,⁷ R. Vazquez Gomez,¹⁹ P. Vazquez Regueiro,³⁹ S. Vecchi,¹⁷ M. van Veghel,⁴³ J. J. Velthuis,⁴⁸ M. Veltri,^{18,r} G. Veneziano,⁴¹ A. Venkateswaran,⁶¹ M. Vernet,⁵ M. Vesterinen,¹² B. Viaud,⁷ D. Vieira,¹ M. Vieites Diaz,³⁹ X. Vilasis-Cardona,^{38,m} V. Volkov,³³ A. Vollhardt,⁴²

B. Voneki,⁴⁰ A. Vorobyev,³¹ V. Vorobyev,^{36,w} C. Voß,⁶⁶ J. A. de Vries,⁴³ C. Vázquez Sierra,³⁹ R. Waldi,⁶⁶ C. Wallace,⁵⁰ R. Wallace,¹³ J. Walsh,²⁴ J. Wang,⁶¹ D. R. Ward,⁴⁹ H. M. Wark,⁵⁴ N. K. Watson,⁴⁷ D. Websdale,⁵⁵ A. Weiden,⁴² M. Whitehead,⁴⁰ J. Wicht,⁵⁰ G. Wilkinson,^{57,40} M. Wilkinson,⁶¹ M. Williams,⁴⁰ M. P. Williams,⁴⁷ M. Williams,⁵⁸ T. Williams,⁴⁷ F. F. Wilson,⁵¹ J. Wimberley,⁶⁰ J. Wishahi,¹⁰ W. Wislicki,²⁹ M. Witek,²⁷ G. Wormser,⁷ S. A. Wotton,⁴⁹ K. Wraight,⁵³ S. Wright,⁴⁹ K. Wyllie,⁴⁰ Y. Xie,⁶⁴ Z. Xing,⁶¹ Z. Xu,⁴¹ Z. Yang,³ H. Yin,⁶⁴ J. Yu,⁶⁴ X. Yuan,^{36,w} O. Yushchenko,³⁷ K. A. Zarebski,⁴⁷ M. Zavertyaev,^{11,c} L. Zhang,³ Y. Zhang,⁷ A. Zhelezov,¹² Y. Zheng,⁶³ A. Zhokhov,³² X. Zhu,³ V. Zhukov,⁹ and S. Zucchelli¹⁵

(LHCb Collaboration)

¹Centro Brasileiro de Pesquisas Físicas (CBPF), Rio de Janeiro, Brazil

²Universidade Federal do Rio de Janeiro (UFRJ), Rio de Janeiro, Brazil

³Center for High Energy Physics, Tsinghua University, Beijing, China

⁴LAPP, Université Savoie Mont-Blanc, CNRS/IN2P3, Annecy-Le-Vieux, France

⁵Clermont Université, Université Blaise Pascal, CNRS/IN2P3, LPC, Clermont-Ferrand, France

⁶CPM, Aix-Marseille Université, CNRS/IN2P3, Marseille, France

⁷LAL, Université Paris-Sud, CNRS/IN2P3, Orsay, France

⁸LPNHE, Université Pierre et Marie Curie, Université Paris Diderot, CNRS/IN2P3, Paris, France

⁹I. Physikalisches Institut, RWTH Aachen University, Aachen, Germany

¹⁰Fakultät Physik, Technische Universität Dortmund, Dortmund, Germany

¹¹Max-Planck-Institut für Kernphysik (MPIK), Heidelberg, Germany

¹²Physikalisches Institut, Ruprecht-Karls-Universität Heidelberg, Heidelberg, Germany

¹³School of Physics, University College Dublin, Dublin, Ireland

¹⁴Sezione INFN di Bari, Bari, Italy

¹⁵Sezione INFN di Bologna, Bologna, Italy

¹⁶Sezione INFN di Cagliari, Cagliari, Italy

¹⁷Sezione INFN di Ferrara, Ferrara, Italy

¹⁸Sezione INFN di Firenze, Firenze, Italy

¹⁹Laboratori Nazionali dell'INFN di Frascati, Frascati, Italy

²⁰Sezione INFN di Genova, Genova, Italy

²¹Sezione INFN di Milano Bicocca, Milano, Italy

²²Sezione INFN di Milano, Milano, Italy

²³Sezione INFN di Padova, Padova, Italy

²⁴Sezione INFN di Pisa, Pisa, Italy

²⁵Sezione INFN di Roma Tor Vergata, Roma, Italy

²⁶Sezione INFN di Roma La Sapienza, Roma, Italy

²⁷Henryk Niewodniczanski Institute of Nuclear Physics Polish Academy of Sciences, Kraków, Poland

²⁸AGH - University of Science and Technology, Faculty of Physics and Applied Computer Science, Kraków, Poland

²⁹National Center for Nuclear Research (NCBJ), Warsaw, Poland

³⁰Horia Hulubei National Institute of Physics and Nuclear Engineering, Bucharest-Magurele, Romania

³¹Petersburg Nuclear Physics Institute (PNPI), Gatchina, Russia

³²Institute of Theoretical and Experimental Physics (ITEP), Moscow, Russia

³³Institute of Nuclear Physics, Moscow State University (SINP MSU), Moscow, Russia

³⁴Institute for Nuclear Research of the Russian Academy of Sciences (INR RAN), Moscow, Russia

³⁵Yandex School of Data Analysis, Moscow, Russia

³⁶Budker Institute of Nuclear Physics (SB RAS), Novosibirsk, Russia

³⁷Institute for High Energy Physics (IHEP), Protvino, Russia

³⁸ICCUB, Universitat de Barcelona, Barcelona, Spain

³⁹Universidad de Santiago de Compostela, Santiago de Compostela, Spain

⁴⁰European Organization for Nuclear Research (CERN), Geneva, Switzerland

⁴¹Ecole Polytechnique Fédérale de Lausanne (EPFL), Lausanne, Switzerland

⁴²Physik-Institut, Universität Zürich, Zürich, Switzerland

⁴³Nikhef National Institute for Subatomic Physics, Amsterdam, The Netherlands

⁴⁴Nikhef National Institute for Subatomic Physics and VU University Amsterdam, Amsterdam, The Netherlands

⁴⁵NSC Kharkiv Institute of Physics and Technology (NSC KIPT), Kharkiv, Ukraine

⁴⁶Institute for Nuclear Research of the National Academy of Sciences (KINR), Kyiv, Ukraine

⁴⁷University of Birmingham, Birmingham, United Kingdom

- ⁴⁸*H.H. Wills Physics Laboratory, University of Bristol, Bristol, United Kingdom*
⁴⁹*Cavendish Laboratory, University of Cambridge, Cambridge, United Kingdom*
⁵⁰*Department of Physics, University of Warwick, Coventry, United Kingdom*
⁵¹*STFC Rutherford Appleton Laboratory, Didcot, United Kingdom*
⁵²*School of Physics and Astronomy, University of Edinburgh, Edinburgh, United Kingdom*
⁵³*School of Physics and Astronomy, University of Glasgow, Glasgow, United Kingdom*
⁵⁴*Oliver Lodge Laboratory, University of Liverpool, Liverpool, United Kingdom*
⁵⁵*Imperial College London, London, United Kingdom*
⁵⁶*School of Physics and Astronomy, University of Manchester, Manchester, United Kingdom*
⁵⁷*Department of Physics, University of Oxford, Oxford, United Kingdom*
⁵⁸*Massachusetts Institute of Technology, Cambridge, Massachusetts, USA*
⁵⁹*University of Cincinnati, Cincinnati, Ohio, USA*
⁶⁰*University of Maryland, College Park, Maryland, USA*
⁶¹*Syracuse University, Syracuse, New York, USA*
⁶²*Pontificia Universidade Católica do Rio de Janeiro (PUC-Rio), Rio de Janeiro, Brazil*
(associated with Universidade Federal do Rio de Janeiro (UFRJ), Rio de Janeiro, Brazil)
⁶³*University of Chinese Academy of Sciences, Beijing, China*
(associated with Center for High Energy Physics, Tsinghua University, Beijing, China)
⁶⁴*Institute of Particle Physics, Central China Normal University, Wuhan, Hubei, China*
(associated with Institution Center for High Energy Physics, Tsinghua University, Beijing, China)
⁶⁵*Departamento de Física, Universidad Nacional de Colombia, Bogota, Colombia*
(associated with Institution LPNHE, Université Pierre et Marie Curie, Université Paris Diderot, CNRS/IN2P3, Paris, France)
⁶⁶*Institut für Physik, Universität Rostock, Rostock, Germany*
(associated with Physikalisches Institut, Ruprecht-Karls-Universität Heidelberg, Heidelberg, Germany)
⁶⁷*National Research Centre Kurchatov Institute, Moscow, Russia*
(associated with Institute of Theoretical and Experimental Physics (ITEP), Moscow, Russia)
⁶⁸*Instituto de Física Corpuscular (IFIC), Universitat de Valencia-CSIC, Valencia, Spain*
(associated with ICCUB, Universitat de Barcelona, Barcelona, Spain)
⁶⁹*Van Swinderen Institute, University of Groningen, Groningen, The Netherlands*
(associated with Nikhef National Institute for Subatomic Physics, Amsterdam, The Netherlands)

[†]Deceased.

^aAlso at Universidade Federal do Triângulo Mineiro (UFTM), Uberaba-MG, Brazil

^bAlso at Laboratoire Leprince-Ringuet, Palaiseau, France

^cAlso at P.N. Lebedev Physical Institute, Russian Academy of Science (LPI RAS), Moscow, Russia

^dAlso at Università di Bari, Bari, Italy

^eAlso at Università di Bologna, Bologna, Italy

^fAlso at Università di Cagliari, Cagliari, Italy

^gAlso at Università di Ferrara, Ferrara, Italy

^hAlso at Università di Genova, Genova, Italy

ⁱAlso at Università di Milano Bicocca, Milano, Italy

^jAlso at Università di Roma Tor Vergata, Roma, Italy

^kAlso at Università di Roma La Sapienza, Roma, Italy

^lAlso at AGH - University of Science and Technology, Faculty of Computer Science, Electronics and Telecommunications, Kraków, Poland

^mAlso at LIFAELS, La Salle, Universitat Ramon Llull, Barcelona, Spain

ⁿAlso at Hanoi University of Science, Hanoi, Viet Nam

^oAlso at Università di Padova, Padova, Italy

^pAlso at Università di Pisa, Pisa, Italy

^qAlso at Università degli Studi di Milano, Milano, Italy

^rAlso at Università di Urbino, Urbino, Italy

^sAlso at Università della Basilicata, Potenza, Italy

^tAlso at Scuola Normale Superiore, Pisa, Italy

^uAlso at Università di Modena e Reggio Emilia, Modena, Italy

^vAlso at Iligan Institute of Technology (IIT), Iligan, Philippines

^wAlso at Novosibirsk State University, Novosibirsk, Russia